

JPP 2010, 62: 47–54  
© 2010 The Authors.  
Journal compilation © 2010  
Royal Pharmaceutical Society  
of Great Britain  
Received June 02, 2009  
Accepted October 05, 2009  
DOI 10.1211/jpp/62.01.0004  
ISSN 0022-3573

## Glucuronidation of piceatannol by human liver microsomes: major role of UGT1A1, UGT1A8 and UGT1A10

Michaela Miksits<sup>a</sup>, Alexandra Maier-Salamon<sup>a</sup>,  
Thanh Phuong Nha Vo<sup>a</sup>, Michael Sulyok<sup>b</sup>, Rainer Schuhmacher<sup>b</sup>,  
Thomas Szekeres<sup>c</sup> and Walter Jäger<sup>a</sup>

<sup>a</sup>Department of Clinical Pharmacy and Diagnostics, University of Vienna, <sup>b</sup>Center for Analytical Chemistry, Department of IFA-Tulln, University of Natural Resources and Applied Life Sciences and <sup>c</sup>Clinical Institute for Medical and Chemical Laboratory Diagnostics, Medical University of Vienna, Vienna, Austria

### Abstract

**Objectives** Piceatannol, a dietary polyphenol present in grapes and wine, is known for its promising anticancer and anti-inflammatory activity. The aim of this study was to analyse the concentration-dependent glucuronidation of piceatannol *in vitro*.

**Methods** To determine the glucuronidation of piceatannol, experiments were conducted with human liver microsomes as well as using a panel of 12 recombinant UDP-glucuronosyltransferase isoforms. Furthermore, the chemical structures of novel glucuronides were identified by liquid chromatography-tandem mass spectrometry (LC-MS/MS).

**Key findings** Along with piceatannol it was possible to identify three metabolites whose structures were identified by LC-MS/MS as piceatannol monoglucuronides (M1–M3). Formation of M1 and M3 exhibited a pattern of substrate inhibition, with apparent  $K_i$  and  $V_{max}/K_m$  values of  $103 \pm 26.6 \mu\text{M}$  and  $3.8 \pm 1.3 \mu\text{l/mg protein per min}$ , respectively, for M1 and  $233 \pm 61.4 \mu\text{M}$  and  $19.8 \pm 9.5 \mu\text{l/mg protein per min}$ , respectively, for M3. In contrast, formation of metabolite M2 followed classical Michaelis–Menten kinetics, with a  $K_m$  of  $18.9 \pm 8.1 \mu\text{M}$  and a  $V_{max}$  of  $0.21 \pm 0.02 \text{ nmol/mg protein per min}$ . Incubation in the presence of human recombinant UDP-glucuronosyltransferases (UGTs) demonstrated that M1 was formed nearly equally by UGT1A1 and UGT1A8. M2 was preferentially catalysed by UGT1A10 and to a lesser extent by UGT1A1 and UGT1A8. The formation of M3, however, was mainly catalysed by UGT1A1 and UGT1A8.

**Conclusions** Our results elucidate the importance of piceatannol glucuronidation in the human liver, which must be taken into account in humans after dietary intake of piceatannol.

**Keywords** glucuronidation; liver; piceatannol; UGT

### Introduction

Piceatannol (3,4,3',5'-tetrahydroxy-*trans*-stilbene, astringinin), a natural resveratrol analogue, is found in a variety of plant sources, such as grapes, red wine, peanuts, rhubarb<sup>[1–3]</sup> and the seeds of *Euphorbia lagascae*.<sup>[4]</sup> Several data demonstrated that resveratrol is metabolised *in vitro* to piceatannol via cytochrome P450 1A2 and 1B1 enzymes,<sup>[5,6]</sup> suggesting resveratrol as a pro-drug for the production of piceatannol. Like resveratrol, piceatannol has been characterized for pharmacological properties, including actions that are anti-inflammatory via inhibiting cyclooxygenase 1 and 2,<sup>[7]</sup> anti-oxidative and immunosuppressive.<sup>[8–11]</sup> Furthermore, piceatannol is a promising chemopreventive agent with anticancer activity against various tumours<sup>[12–14]</sup> and, as demonstrated in recent experiments on human HL-60 promyelocytic leukaemia cells, also pronounced inhibition of ribonucleotide reductase, inhibition of cell cycle progression, induction of apoptosis and synergism with Ara-C.<sup>[15]</sup>

Until recently, little was known of piceatannol metabolism *in vitro*. A study in our laboratory demonstrated that piceatannol is sulfated in human liver cytosol to two monosulfates and one disulfate.<sup>[16]</sup> Additionally, these findings showed that the sulfation of the polyphenol is mainly catalysed by the cytosolic sulfotransferases (SULTs) 1A1\*1, 1A2\*1, 1B1 and 1E1. In rats, however, Roupe *et al.*<sup>[17]</sup> showed that piceatannol is

**Correspondence:** Dr Walter Jäger, Department of Clinical Pharmacy and Diagnostics, University of Vienna, Althanstrasse 14, A-1090 Vienna, Austria.  
E-mail: walter.jaeger@univie.ac.at

exclusively metabolised to two structurally unknown glucuronides. Rapid glucuronidation is also consistent with previous studies of resveratrol in rodents and humans, which have predominantly shown glucuronides but less sulfates in plasma and urine after oral application.<sup>[18,19]</sup> The pattern of metabolite formation, however, is strongly influenced by dose, as recently demonstrated in our laboratory using human intestinal Caco-2 cells and rat isolated perfused livers. In both models, we showed that sulfation prevailed at the lower resveratrol concentrations; when the applied dose was raised, however, sulfate formation dropped dramatically. As a consequence of the observed decreased formation of resveratrol sulfates by substrate inhibition, conjugation with glucuronic acid was the main metabolic pathway at higher resveratrol concentrations.<sup>[20,21]</sup>

Glucuronidation represents a major conjugation reaction that involves the transfer of a glucuronyl moiety from the ubiquitous co-substrate UDP-glucuronic acid (UDPGA) to non-polar substrates by a family of enzymes known as the UDP-glucuronosyltransferases (UGTs). It is an important pathway for endogenous as well as numerous exogenous compounds, drugs and dietary constituents.<sup>[22]</sup> To date, however, no enzymatic study on the formation of piceatannol glucuronides has been performed in either the rat or human liver. So far, it is known that glucuronidation of the structural analogue resveratrol is mainly catalysed by the UDP-glucuronosyltransferases UGT1A1 and UGT1A9, forming resveratrol-3-O-glucuronide and to a lesser extent resveratrol-4'-O-glucuronide.<sup>[23]</sup> Recently, Iwuchukwu and Nagar<sup>[24]</sup> observed atypical kinetic profiles for the formation of these two main resveratrol conjugates by UGT1A1 and UGT1A9. As we recently demonstrated that piceatannol sulfation also displays atypical metabolic profiles in human liver cytosol and recombinant sulfotransferases,<sup>[16]</sup> complex enzyme kinetics must be considered as well for piceatannol glucuronide formation.

The purpose of this study was to identify the possible roles of human UGT isoforms in piceatannol glucuronidation by kinetic analysis using recombinant UGTs in addition to human liver microsomes. Furthermore, the chemical structures of glucuronides should be elucidated by liquid chromatography-tandem mass spectrometry (LC-MS/MS).

## Materials and Methods

### Materials

Piceatannol (*trans*-3,4,3',5'-tetrahydroxystilbene),  $\beta$ -glucuronidase type B-3 from bovine liver, uridine 5'-diphosphoglucuronic acid (UDPGA, 98–100% purity) and dimethyl sulfoxide (DMSO) were obtained from Sigma-Aldrich (Munich, Germany). Methanol and water were of HPLC grade (Merck, Darmstadt, Germany). Human liver microsomes (protein content 20 mg/ml in 250 mM sucrose) from one male and two females (ages 65, 45 and 78 years) and baculovirus-infected insect cells containing the cDNA for human UGTs 1A1, 1A3, 1A4, 1A6, 1A7, 1A8, 1A9, 1A10, 2B4, 2B7, 2B15 and 2B17 were obtained from BD Biosciences (Woburn, USA). The catalytic activity of human liver microsomes and recombinant UGTs were as described in the data sheets

provided by the manufacturer. All other chemicals and solvents were commercially available, of analytical grade and used without further purification.

### Metabolism of piceatannol by human liver microsomes

Five microlitres of human liver microsomes (0.5 mg protein/ml, final concentration) and Brij 58 (100  $\mu$ g/mg protein) were pre-incubated on ice for 30 min. Afterwards, magnesium chloride (10 mM), D-saccharic acid-1,4-lactone (5 mM) and piceatannol (final concentration 10–2000  $\mu$ M) in DMSO were added to 50 mM potassium phosphate buffer (pH 7.4) in a total volume of 100  $\mu$ l. Reactions were initiated by the addition of 3 mM UDPGA, and the samples were incubated for 60 min at 37°C. Control experiments in the absence of UDPGA were run in parallel. After the reactions had been terminated by the addition of 200  $\mu$ l methanol, the samples were centrifuged (13 000 g for 5 min); a total of 80  $\mu$ l of the supernatant was injected onto the HPLC column. The mobile phase and gradient were determined by HPLC as described previously<sup>[14]</sup> using a Dionex 'UltiMate 3000' system (Dionex Corp., Sunnyvale, USA). Chromatographic separation of piceatannol and its metabolites was performed on a Hypersil BDS-C<sub>18</sub> column (5  $\mu$ m, 250 × 4.6 mm i.d.; Thermo Fisher Scientific, Inc, Waltham, USA), preceded by a Hypersil BDS-C<sub>18</sub> precolumn (5  $\mu$ m, 10 × 4.6 mm i.d.), at a flow rate of 1 ml/min. Calibration of the chromatogram was accomplished using the external standard method. As standards of the metabolites were not available, quantification of metabolite concentrations was based on the assumption that the unknown metabolites had molar extinction coefficients similar to that of piceatannol. Linear calibration curves were derived from the peak area of piceatannol and its metabolites to the external standard piceatannol using standard solutions of piceatannol, to yield a concentration range of 0.05–100  $\mu$ g/ml. Linear regression analysis of the standard curve showed a correlation coefficient of  $r^2 = 0.999$ . The accuracy of the assay (mean error, %) at the lowest concentrations of substrate was assessed by three replicate analysis of microsomal samples with known amounts of piceatannol. The inter-day values for the glucuronide conjugates M1–M3 at 1  $\mu$ M ranged from 6.4% to 10.8%, and the intra-assay variability ranged from 4.1% to 9.2%.

### Effect of detergents on piceatannol glucuronidation by human liver microsomes

UGT proteins are located in the endoplasmic reticulum and are subject to latency of their enzymatic activity. This has resulted in the use of detergents to obtain the maximal activity by disrupting the integrity of the membranes.<sup>[25]</sup> We therefore examined the effect of low solubilising concentrations of some common detergents on the catalytic activity of UGTs involved in piceatannol glucuronidation.

Five microlitres of human liver microsomes (0.5 mg protein/ml, final concentration) were pre-incubated with 25, 50 or 100  $\mu$ g Triton X-100 as well as Brij 35, Brij 58, alamethicin and digitonin/mg microsomal protein on ice for 30 min. Then, magnesium chloride (10 mM), D-saccharic

acid-1,4-lactone (5 mM) and piceatannol (final concentration 80  $\mu\text{M}$ ) in DMSO were added to 50 mM potassium phosphate buffer (pH 7.4) in a total volume of 100  $\mu\text{l}$ . The glucuronidation assay was then initiated by adding 3 mM UDPGA, and the metabolism of piceatannol was assessed after a 60-min incubation at 37°C as described above. Control experiments in the absence of detergent were run in parallel.

### Glucuronidation of piceatannol by human recombinant UDP-glucuronosyltransferase isoenzymes

To assay piceatannol metabolites, microsomes (0.25 mg protein/ml, final concentration) prepared from baculovirus-infected insect cells (BTI-TN-5B1-4; containing the cDNA for human UGT 1A1, 1A3, 1A4, 1A6, 1A7, 1A8, 1A9, 1A10, 2B4, 2B7, 2B15 and 2B17, respectively) were incubated at 37°C for 60 min with piceatannol (40  $\mu\text{M}$ ), UDPGA (3 mM), Brij 58 (100  $\mu\text{g}/\text{mg}$  protein) and 50 mM  $\text{KH}_2\text{PO}_4$  buffer (pH 7.4). Assays were performed in triplicate in a final volume of 100  $\mu\text{l}$ . Reactions were terminated by the addition of 200  $\mu\text{l}$  methanol and centrifuged at 13 000  $g$  for 5 min, and 100  $\mu\text{l}$  of the clear supernatant was applied onto an HPLC column. Glucuronidation of piceatannol was not observed when using insect cells infected with wild type baculovirus (*Autographa californica*). Enzyme kinetics for glucuronidation by UGT1A1, UGT1A8 and UGT1A9 were evaluated by incubation of the recombinant enzymes (0.25 mg protein/ml) with piceatannol (10–2000  $\mu\text{M}$ ) under conditions identical to those mentioned above.

### Identification of piceatannol metabolites

After a 60 min incubation of human liver microsomes or recombinant UGTs, 2  $\mu\text{l}$  of glucuronidase (200 U) was added to 100  $\mu\text{l}$  of the reaction mixtures and was further incubated at 37°C for 60 min. The reactions were stopped by the addition of methanol, and the samples were analysed as mentioned above. To distinguish between mono- and diglucuronidation of piceatannol, liquid chromatography-mass spectrometry (LC-MS) measurements were performed with an 1100 Series HPLC system (Agilent, Waldbronn, Germany) coupled to a G1315B DAD detector and QTrap 4000 LC-MS/MS system (Applied Biosystems, Foster City, USA) equipped with a TurboIonSpray ESI source. ESI-MS/MS was performed in negative polarity with the following settings: source temperature 550°C, curtain gas 10 psi (99.5% nitrogen), ion source gas 1 (sheath gas) 30 psi, ion source gas 2 (drying gas) 50 psi, ion spray voltage –4000 V, and collision gas (nitrogen) high. The optimisation of the analyte-dependent MS/MS parameters was performed by direct infusion of piceatannol (dissolved in 1 ml methanol) into the mass spectrometer using a 11 Plus syringe pump (Harvard Apparatus, Holliston, USA). The injection volume was 20  $\mu\text{l}$ . The column, mobile phase, gradient and flow rate were identical to those used for the analytical HPLC assay (see above).

### Data analysis

Each incubation step in the various glucuronidation assays was performed at least in triplicate and the results were expressed as means  $\pm$  SD. Formation rates calculated for the recombinant enzymes were mathematically adjusted to the individual glucuronidation activity of the microsomes, as given by the company. The data were fitted to Michaelis–Menten (hyperbolic) and substrate inhibition models and further analysed using Eadie–Hofstee plots. The coefficient of determination ( $R^2$ ) and visual inspection of the Eadie–Hofstee plots were used to determine the quality of a fit to a specific model. Kinetic parameters were estimated using the Prism program (version 5.0; GraphPad Software Inc., San Diego, USA) for Michaelis–Menten (Equation 1) and substrate inhibition kinetics (Equation 2):

$$V = V_{\max} \cdot S / (K_m + S) \quad (1)$$

$$V = V_{\max} / (1 + K_m / S + S / K_i) \quad (2)$$

where  $V$  is the rate of reaction,  $V_{\max}$  the maximum velocity,  $K_m$  the Michaelis constant,  $S$  the substrate concentration and  $K_i$  the inhibition constant. The enzymatic efficacy, which is defined as the  $V_{\max}/K_m$  ratio, quantifies the glucuronidation capacity and corresponds to the intrinsic clearance. The statistical significance for the effect of detergents on the metabolite formation in human liver microsomes was calculated by applying the one-way analysis of variance for multiple comparisons. The Tukey's post-hoc comparisons were used to determine the source of significance where appropriate.  $P < 0.05$  was considered statistically significant.

## Results

### Piceatannol metabolism in human liver microsomes

Liver microsomes from three individual human livers were incubated with piceatannol (20  $\mu\text{M}$ ) for 60 min and subsequently analysed by HPLC. A typical HPLC chromatogram from these experiments is shown in Figure 1. In the presence of UDPGA, three metabolites were detected in addition to piceatannol ( $t_r = 30.5$  min): M1 ( $t_r = 17.8$  min), M2 ( $t_r = 19.5$  min), and M3 ( $t_r = 23.2$  min).

### Effect of detergents on piceatannol glucuronidation by human liver microsomes

Human liver microsomes were pre-treated with increasing concentrations of Triton X-100, digitonin, Brij 58, Brij 35 and alamethicin (0–100  $\mu\text{g}$  of detergent/mg of protein) for 30 min before the addition of the reaction mixture. Control experiments in the absence of detergents were run in parallel. At 25  $\mu\text{g}/\text{mg}$  protein, all examined detergents, with the exception of Triton X-100, increased M2 formation from 1.0% (alamethicin) to 30.7% (Brij 58) compared with the non-detergent control (Figure 2). Except for alamethicin, a further increase of detergent concentration to 50  $\mu\text{g}/\text{mg}$  protein again increased M2 glucuronidation; the highest increase in M2 formation (2.3 fold) was observed with Brij 58 as the detergent. When the detergent concentration was

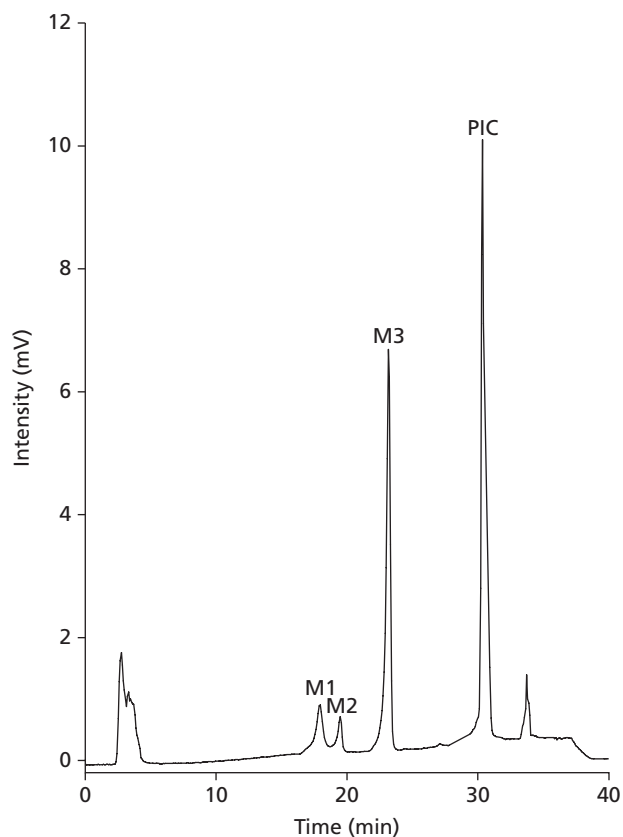


**Figure 1** Representative HPLC chromatogram of piceatannol (PIC; 20  $\mu\text{M}$ ) and its three metabolites (M1–M3) in human liver microsomes. For details, see the Materials and Methods section.

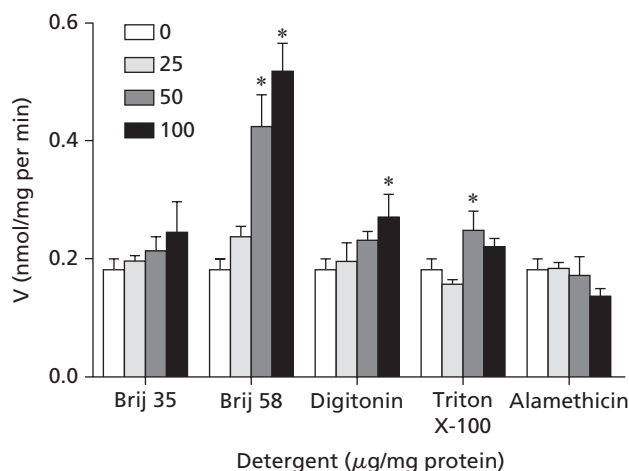


**Figure 2** Effect of detergents on the formation of M2 in human liver microsomes. For details, see the Material and Methods section. \* $P < 0.05$  compared with control.

raised to 100  $\mu\text{g}/\text{mg}$  protein, only Brij 35 (17.6%), digitonin (27.5%) and Brij 58 (33.0%) again showed stimulation of piceatannol glucuronidation. Since Brij 58 showed the highest glucuronidation rates, it was therefore the detergent of choice for studying piceatannol glucuronidation *in vitro*.

Qualitatively similar detergent-dependent metabolic profiles for M1 and M3 formation were found.

### Kinetics of piceatannol glucuronidation in human liver microsomes

The formation of M1–M3 in human liver microsomes was linear with respect to both time (up to 300 min) and microsomal protein concentrations (0.25–2 mg/ml). Figure 3 shows the glucuronidation of piceatannol along with Eadie–Hofstee plots. The large variability in piceatannol glucuronidation is due to great inter-individual differences in the catalytic activity of UGTs of the three used human liver microsomes. The kinetic constants for these reactions were estimated using piceatannol concentrations of 1–2000  $\mu\text{M}$  (see Table 1).

As shown in Figure 3b, the formation of the minor metabolite M2 followed classical Michaelis–Menten kinetics (Equation 1) ( $R^2 = 0.51$ ). This kinetic model was confirmed by a linear Eadie–Hofstee plot.<sup>[26]</sup> In contrast to M2, the apparent enzyme kinetic parameters for M1 and M3 were estimated by fitting to the substrate inhibition equation (Equation 2) (M1:  $R^2 = 0.54$ ; M3:  $R^2 = 0.45$ ). The substrate inhibition profile was confirmed by a curved Eadie–Hofstee plot (Figure 3a, c).

### Glucuronidation of piceatannol by recombinant UDP-glucuronosyltransferases

The structure of piceatannol suggests that one or more of the human UGTs involved in phenol or oestrogen conjugation may readily glucuronidate this compound. Therefore, twelve single recombinant human UGT microsomes from insect cells were also incubated with piceatannol (40  $\mu\text{M}$ ) for 60 min after pre-treatment with the solubilising agent Brij 58. This initial screening showed that UGT1A1, 1A3, 1A6, 1A7, 1A8, 1A9, 1A10, 2B7 and 2B15 glucuronidated piceatannol to varying extents to up to three metabolites (Figure 4). Among these isoforms, the formation of M1 was preferentially catalysed by UGT1A8 (49.2%;  $126.6 \pm 0.3$  pmol/mg per min) and UGT1A1 (42.1%;  $108.6 \pm 2.6$  pmol/mg per min) but reached only 5.2% by UGT1A9. M2 was mainly formed by UGT1A10 (54.7%;  $1333 \pm 77.2$  pmol/mg per min), 1A1 (22.2%;  $541.6 \pm 47.8$  pmol/mg per min) and 1A3 (11.8%;  $288.8 \pm 3.2$  pmol/mg per min) and only to a minor extent (8.5%) by UGT1A8. UGT1A7, 1A9 and 2B7 each only contributed to  $\leq 2\%$  of the total M2 glucuronidation. The formation of M3 was mainly catalysed by UGT1A1 (34.6%;  $1067 \pm 107.9$  pmol/mg per min), UGT1A8 (30.9%;  $951.6 \pm 25.7$  pmol/mg per min) and UGT1A10 (18.0%;  $555.0 \pm 32.1$  pmol/mg per min), whereas UGT1A3, 1A6, 1A7, 1A9, 2B7 and 2B15 exhibited low catalytic activity for the formation of M3. No detectable formation of M1–M3 was seen with UGT1A4, 2B4 or 2B17.

### Kinetics of piceatannol glucuronidation in recombinant UGT1A1, 1A8 and 1A10

A comparative kinetic analysis was performed using piceatannol concentrations in the range 1–2000  $\mu\text{M}$  to investigate, in greater detail, the catalytic activity of UGT1A1, 1A8 and 1A10 for piceatannol glucuronidation.

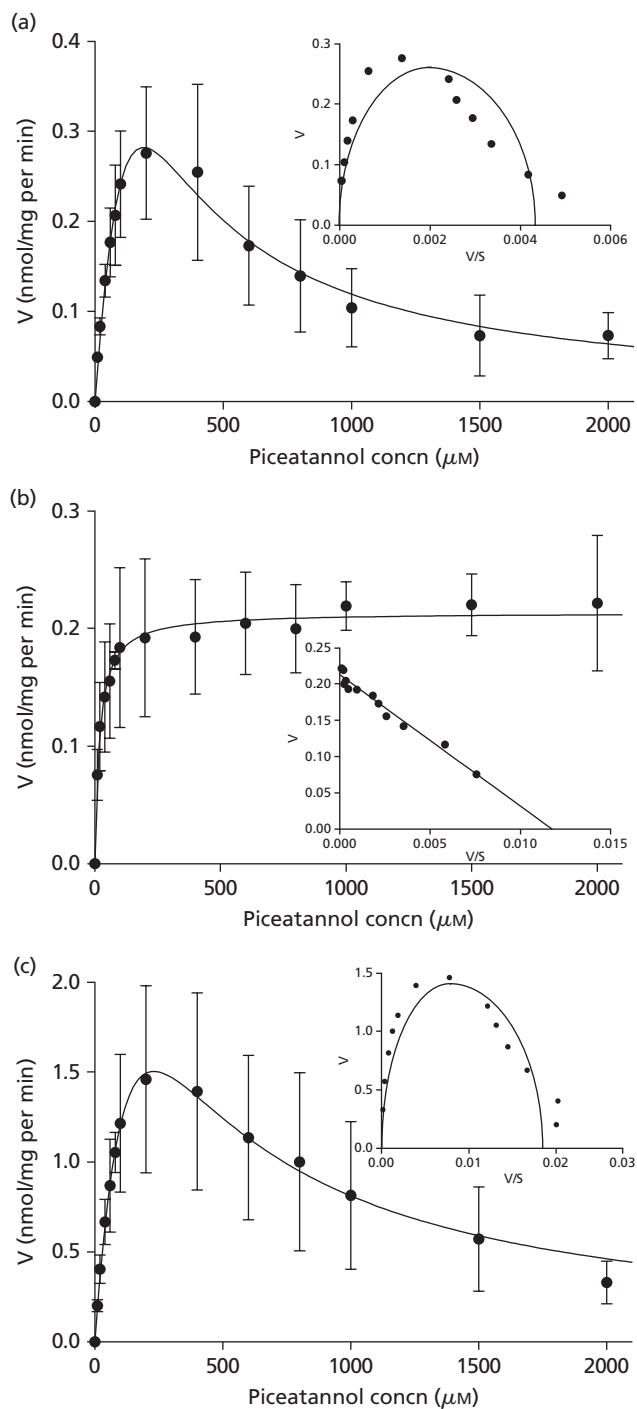


**Figure 3** Kinetics of M1 (a), M2 (b) and M3 (c) formation in human liver microsomes normalised to protein content as a function of piceatannol concentration. Eadie-Hofstee plots are shown as insets on each graph. Human liver microsomes were incubated with piceatannol for 60 min at 37°C in the presence of UDPGA. Data are expressed as means  $\pm$  SD,  $n = 3$ , of individual preparations.

The apparent enzyme kinetic parameters for M1–M3 of the three recombinant isoenzymes were estimated by fitting to the substrate inhibition model (Equation 2). Kinetic data are reported in Table 2.

The maximal velocity of formation ( $V_{\max}$ ) of M1 was significantly lower for UGT1A1 than UGT1A8.  $K_i$  values also differed significantly between these two investigated UGT isoenzymes. Interestingly, the UGT with the highest  $V_{\max}$  value showed a lower  $K_i$  estimate. The kinetic parameters of M1 formation by recombinant human UGT1A10 were below the detection limit.

The formation of M2 resulted in a slightly higher (1.1 and 1.3 fold)  $K_m$  value but significantly higher (2.6 and 7.9 fold)  $V_{\max}$  value for UGT1A10 than UGT1A1 and UGT1A8, respectively. Additionally, the  $V_{\max}/K_m$  values of UGT1A10 were 2.3- and 5.9-fold higher than those for the other two UGT isoenzymes. Among these recombinant isoforms, UGT1A1 and UGT1A10 showed nearly the same  $K_i$  estimates, whereas the  $K_i$  value of UGT1A8 was 5.3-fold higher.

The comparison of the M3 formation kinetic estimates revealed high  $K_m$  and  $V_{\max}$  estimates for UGT1A1 and UGT1A8 compared with those for the UGT1A10 isoenzyme. However, UGT1A10 showed the highest  $V_{\max}/K_m$  and  $K_i$  values.

### Identification of piceatannol metabolites

Treatment of samples with  $\beta$ -glucuronidase before HPLC analysis led to the disappearance of M1, M2 and M3. The concomitant increase of parent piceatannol indicates glucuronidation of all three metabolites. Structural identification of piceatannol glucuronides was confirmed by LC-MS/MS. Negative ion mass spectra of piceatannol and its three biotransformation products showed stable molecular ions at  $m/z = 243$  and  $m/z = 419$  amu, with subsequent loss of 176 amu (glucuronic acid moiety) for M1–M3; these findings are in agreement with the molecular weight of piceatannol and piceatannol monoglucuronides. Based on mass spectra, however, it was not possible to determine the point of attachment for glucuronidation. Due to insufficient amounts of the metabolites M1–M3 in the incubation media and as authentic standards were not available it was not possible to determine the exact structure of piceatannol metabolites by NMR. Figure 5 shows the proposed metabolic pathway of piceatannol by human liver microsomes and recombinant human UGTs.

### Discussion

Glucuronidation is a major drug-metabolising reaction in humans and accounts for approximately 40–70% of xenobiotic elimination.<sup>[27]</sup> All classes of drugs are substrates for this pathway. The process, mediated by the family of UDP-glucuronosyltransferase enzymes (UGTs), increases the polarity of hydrophobic compounds and results, in many cases, in loss of biological activity. UGTs also play a role in the generation of bioactive compounds. Morphine-6-glucuronide,<sup>[28]</sup> retinoyl  $\beta$ -glucuronide and retinyl  $\beta$ -glucuronide,<sup>[29]</sup> and digitoxin- and digoxin-glucuronides,<sup>[30]</sup> in particular, are known to have pharmacological or toxicological activity equivalent to (or unique compared with) their parent aglycones.

This is the first study that provides a detailed investigation of the metabolism of in-vitro glucuronidation of piceatannol

**Table 1** Kinetic parameters of M1–M3 formation in human liver microsomes

Metabolite	Model	$K_m$ ( $\mu\text{M}$ )	$V_{\text{max}}$ (nmol/mg protein per min)	$V_{\text{max}}/K_m$ ( $\mu\text{l}/\text{min}$ per mg)	$K_i$ ( $\mu\text{M}$ )
M1	Substrate inhibition	$346 \pm 40.2$	$1.3 \pm 0.8$	$3.8 \pm 1.3$	$103 \pm 26.6$
M2	Michaelis–Menten	$18.9 \pm 8.1$	$0.21 \pm 0.02$	$11.1 \pm 4.7$	n.a.
M3	Substrate inhibition	$227 \pm 178$	$4.5 \pm 2.4$	$19.8 \pm 9.5$	$233 \pm 61.4$

Data are shown as means  $\pm$  SD of three determinations. n.a., not applicable.

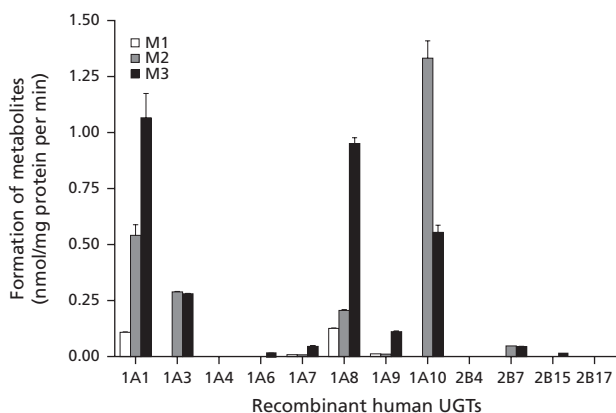


**Figure 4** Rate of M1–M3 formation in recombinant human UDP-glucuronosyltransferases (UGTs) normalised to protein content as a function of piceatannol concentration. Recombinant human UGTs were incubated with  $40 \mu\text{M}$  piceatannol for 60 min at  $37^\circ\text{C}$  in the presence of UDPGA. Data are shown as means  $\pm$  SD of three determinations.

by human liver microsomes as well as the specific UGT isoforms responsible for the formation of piceatannol glucuronides. So far, preliminary experiments by Roupe and co-workers<sup>[17]</sup> have revealed two piceatannol glucuronides in rat plasma after intravenous administration of 10 mg/kg piceatannol. The same two metabolites were also determined by the same authors in in-vitro samples in rat liver microsomes, which were incubated with piceatannol as a parent drug. In our study, piceatannol was extensively metabolised in the human liver to three conjugates (mono-glucuronides) identified by LC-MS/MS analysis and enzymatic hydrolysis with glucuronidases. The formation of M1

and M3 clearly prevailed at lower substrate concentrations of 1–200  $\mu\text{M}$ . At concentrations greater than 200  $\mu\text{M}$  piceatannol, however, substrate inhibition was observed. M2 formation followed classical Michaelis–Menten kinetics, resulting in significantly lower  $V_{\text{max}}$  and  $K_m$  values.

In this study, glucuronidation of piceatannol was evaluated using all currently available UGT isoforms. The main UGT isoforms catalysing the glucuronidation of this compound are UGT1A1, UGT1A8 and UGT1A10. Among these screened enzymes the kinetic profiles for all three glucuronides were similar to one another, differing only in their rates of formation ( $K_m$ ,  $V_{\text{max}}$ ) and substrate inhibition ( $K_i$ ). The formation of M1 is preferentially catalysed by UGT1A8 ( $0.57 \pm 0.17$  nmol/mg protein per min), whereas M2 is mainly formed by UGT1A10 ( $2.6 \pm 0.63$  nmol/mg protein per min). UGT1A1 ( $3.0 \pm 0.73$  nmol/mg protein per min) and UGT1A8 ( $4.3 \pm 1.6$  nmol/mg protein per min) contributed equally to the formation of metabolite M3. UGT1A3, 1A6, 1A7, 1A9, 2B7 and 2B15 were also capable of piceatannol glucuronidation, but they exhibited only low catalytic activity. Furthermore, our data demonstrated hepatic as well as extrahepatic glucuronidation of piceatannol. UGT1A1 has been observed in the liver and small intestine, whereas 1A8 and 1A10 are expressed in the human colon but not human liver.<sup>[22]</sup> During absorption, piceatannol may therefore be glucuronidated by several intestinal UGT isoenzymes that may contribute to piceatannol metabolism.

However, Roupe and colleagues<sup>[17]</sup> found only two piceatannol glucuronides in rat liver microsomes. This discrepancy may be due to species-specific differences or the use of alamethicin as a solubilising agent. Pre-treatment of liver microsomes and the recombinant UGT isoforms with increasing concentrations of solubilising agents demonstrated

**Table 2** Kinetic parameters of M1–M3 formation by recombinant human UGT1A1, UGT1A8 and UGT1A10

Metabolite	$K_m$ ( $\mu\text{M}$ )	$V_{\text{max}}$ (nmol/mg protein per min)	$V_{\text{max}}/K_m$ ( $\mu\text{l}/\text{min}$ per mg)	$K_i$ ( $\mu\text{M}$ )
UGT1A1	M1	$8.2 \pm 1.5$	$0.13 \pm 0.01$	$15.9 \pm 4.7$
	M2	$30.1 \pm 7.2$	$0.97 \pm 0.13$	$104 \pm 21.6$
	M3	$73.7 \pm 28.4$	$3.0 \pm 0.73$	$149 \pm 51.6$
UGT1A8	M1	$87.5 \pm 39.5$	$0.57 \pm 0.17$	$114 \pm 46.3$
	M2	$25.9 \pm 4.7$	$0.33 \pm 0.02$	$560 \pm 81.6$
	M3	$110 \pm 53.3$	$4.3 \pm 1.6$	$48.2 \pm 22.2$
UGT1A10	M1	n.d.	n.d.	n.d.
	M2	$34.1 \pm 14.8$	$2.6 \pm 0.63$	$106 \pm 41.4$
	M3	$16.9 \pm 4.6$	$0.82 \pm 0.08$	$380 \pm 79.1$

Data are shown as means  $\pm$  SD of three determinations. The apparent enzyme kinetic parameters were estimated by fitting to the substrate inhibition equation (Equation 2). n.d., not detected.

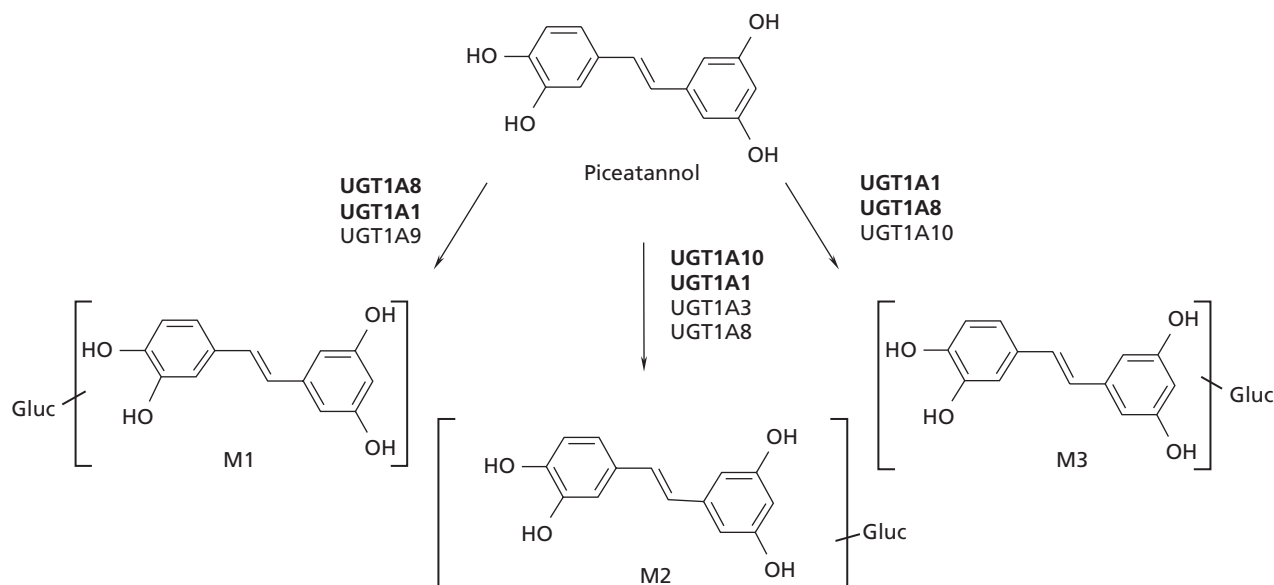


**Figure 5** Proposed metabolic pathway for piceatannol ( $40 \mu\text{M}$ ) by human liver microsomes and recombinant human UDP-glucuronosyltransferases (UGTs). UGT enzymes shown in bold are those that contribute most to glucuronide formation.

that the choice of detergent and its applied concentration has a significant influence on piceatannol glucuronidation rates. Using 50 and 100  $\mu\text{g}$  Brij 58/mg protein, we found a significant stimulation ( $P < 0.05$ ) of the catalytic activity of the UGTs compared with control experiments performed without former activation. However, application of alame-thicin even led to inhibition of piceatannol glucuronidation to levels reaching 64–80% of control values. When using solubilising agents for the study of in-vitro piceatannol glucuronidation, therefore, the choice of detergent and its concentration may be crucial for the results of the experiments.

It is not known yet whether piceatannol conjugates also exhibit pharmacological activity. However, numerous studies have shown that glucuronides can accumulate during chronic therapy.<sup>[31–33]</sup> Cleavage of the glucuronides by human  $\beta$ -glucuronidase, an enzyme expressed in many tissues and body fluids in humans, can release the parent compounds and thereby modify drug disposition.<sup>[34]</sup> Therefore, piceatannol conjugates may also serve as inactive pools for piceatannol. Conjugation might also prevent piceatannol from enzymatic oxidation, extending its half-life in the cell and maintaining its biological properties.<sup>[35]</sup>

## Conclusions

Our data demonstrated that piceatannol is extensively metabolised in human liver microsomes to three monoglucuronides by liver specific UGT1A1 and intestinal UGT1A8 and UGT1A10, which may also apply to human hepatocytes and enterocytes. Glucuronidation will therefore play a key role in the elimination of piceatannol in humans after oral uptake of dietary piceatannol, strongly affecting bioavailability. Measurements of both parent and glucuronide species will be necessary to correlate pharmacokinetic with pharmacological activity.

## Declarations

### Conflict of interest

The Author(s) declare(s) that they have no conflicts of interest to disclose.

### Funding

This study was supported by grants from the Jubiläumsfonds der Österreichischen Nationalbank (12600 to W.J.) and ‘Medizinisch-Wissenschaftlicher Fonds des Bürgermeisters der Bundeshauptstadt Wien’ (2296; T.S.)

## References

- Bavaresco L. Role of viticultural factors on stilbene concentrations of grapes and wine. *Drugs Exp Clin Res* 2003; 29: 181–187.
- Ku KL *et al.* Production of stilbenoids from the callus of *Arachis hypogaea*: a novel source of the anticancer compound piceatannol. *J Agric Food Chem* 2005; 53: 3877–3881.
- Matsuda H *et al.* Effects of stilbene constituents from rhubarb on nitric oxide production in lipopolysaccharide-activated macrophages. *Bioorg Med Chem Lett* 2000; 10: 323–327.
- Ferrigni NR *et al.* Use of potato disc and brine shrimp bioassays to detect activity and isolate piceatannol as the antileukemic principle from the seeds of *Euphorbia lagascae*. *J Nat Prod* 1984; 47: 347–352.
- Piver B *et al.* Involvement of cytochrome P450 1A2 in the biotransformation of trans-resveratrol in human liver microsomes. *Biochem Pharmacol* 2004; 68: 773–782.
- Potter GA *et al.* The cancer preventative agent resveratrol is converted to the anticancer agent piceatannol by the cytochrome P450 enzyme CYP1B1. *Br J Cancer* 2002; 86: 774–778.
- Murias M *et al.* Resveratrol analogues as selective cyclooxygenase-2 inhibitors: synthesis and structure-activity relationship. *Bioorg Med Chem* 2004; 12: 5571–5578.



8. Wiedner T *et al.* Piceatannol, a hydroxylated analog of the chemopreventive agent resveratrol, is a potent inducer of apoptosis in the lymphoma cell line BJAB and in primary, leukemic lymphoblasts. *Leukemia* 2001; 15: 1735–1742.
9. Seow CJ *et al.* Piceatannol, a Syk-selective tyrosine kinase inhibitor, attenuated antigen challenge of guinea pig airways in vitro. *Eur J Pharmacol* 2002; 443: 189–196.
10. Murias M *et al.* Antioxidant, prooxidant and cytotoxic activity of hydroxylated resveratrol analogues: structure-activity relationship. *Biochem Pharmacol* 2005; 69: 903–912.
11. Ovesná Z *et al.* Antioxidant activity of resveratrol, piceatannol and 3,3',4,4',5,5'-hexahydroxy-trans-stilbene in three leukemia cell lines. *Oncol Rep* 2006; 16: 617–624.
12. Wolter F *et al.* Piceatannol, a natural analog of resveratrol, inhibits progression through the S phase of the cell cycle in colorectal cancer cell lines. *J Nutr* 2002; 132: 298–302.
13. Larrosa M *et al.* The grape and wine polyphenol piceatannol is a potent inducer of apoptosis in human SK-Mel-28 melanoma cells. *Eur J Nutr* 2004; 43: 275–284.
14. Kuo PL, Hsu YL. The grape and wine constituent piceatannol inhibits proliferation of human bladder cancer cells via blocking cell cycle progression and inducing Fas/membrane bound Fas ligand-mediated apoptotic pathway. *Mol Nutr Food Res* 2008; 52: 408–418.
15. Fritzer-Szekeres M *et al.* Biochemical effects of piceatannol in human HL-60 promyelocytic leukemia cells - synergism with Ara-C. *Int J Oncol* 2008; 33: 887–892.
16. Miksits M *et al.* In-vitro sulfation of piceatannol by human liver cytosol and recombinant sulfotransferases. *J Pharm Pharmacol* 2009; 61: 185–191.
17. Roupe K *et al.* Determination of piceatannol in rat serum and liver microsomes: pharmacokinetics and phase I and II biotransformation. *Biomed Chromatogr* 2004; 18: 486–491.
18. Walle T *et al.* High absorption but very low bioavailability of oral resveratrol in humans. *Drug Metab Dispos* 2004; 32: 1377–1382.
19. Wenzel E, Somoza V. Metabolism and bioavailability of trans-resveratrol. *Mol Nutr Food Res* 2005; 49: 472–481.
20. Maier-Salamon A *et al.* Increased transport of resveratrol across monolayers of the human intestinal Caco-2 cells is mediated by inhibition and saturation of metabolites. *Pharm Res* 2006; 23: 2107–2115.
21. Maier-Salamon A *et al.* Metabolism and disposition of resveratrol in the isolated perfused rat liver: role of Mrp2 in the biliary excretion of glucuronides. *J Pharm Sci* 2008; 97: 1615–1628.
22. King CD *et al.* UDP-glucuronosyltransferases. *Curr Drug Metab* 2000; 1: 143–161.
23. Aumont V *et al.* Regioselective and stereospecific glucuronidation of trans- and cis-resveratrol in human. *Arch Biochem Biophys* 2001; 393: 281–289.
24. Iwuchukwu OF, Nagar S. Resveratrol (trans-resveratrol, 3,5,4'-trihydroxy-trans-stilbene) glucuronidation exhibits atypical enzyme kinetics in various protein sources. *Drug Metab Dispos* 2008; 36: 322–330.
25. Soars MG *et al.* The effect of incubation conditions on the enzyme kinetics of udp-glucuronosyltransferases. *Drug Metab Dispos* 2003; 31: 762–767.
26. Hutzler JM, Tracy TS. Atypical kinetic profiles in drug metabolism reactions. *Drug Metab Dispos* 2002; 30: 355–362.
27. Wells PG *et al.* Glucuronidation and the UDP-glucuronosyltransferases in health and disease. *Drug Metab Dispos* 2004; 32: 281–290.
28. Romberg R *et al.* Pharmacokinetic-pharmacodynamic modeling of morphine-6-glucuronide-induced analgesia in healthy volunteers: absence of sex differences. *Anesthesiology* 2004; 100: 120–133.
29. Olson JA *et al.* Enhancement of biological activity by conjugation reactions. *J Nutr* 1992; 122: 615–624.
30. Scholz H, Schmitz W. Positive inotropic effects of digitoxin- and digoxin-glucuronide in human isolated ventricular heart muscle preparations. *Basic Res Cardiol* 1984; 79: 134–139.
31. Fromm MF *et al.* Influence of renal function on the steady-state pharmacokinetics of the antiarrhythmic propafenone and its phase I and phase II metabolites. *Eur J Clin Pharmacol* 1995; 48: 279–283.
32. Grubb NG *et al.* Stereoselective pharmacokinetics of ketoprofen and ketoprofen glucuronide in end-stage renal disease: evidence for a 'futile cycle' of elimination. *Br J Clin Pharmacol* 1999; 48: 494–500.
33. MacPhee IA *et al.* Pharmacokinetics of mycophenolate mofetil in patients with end-stage renal failure. *Kidney Int* 2000; 57: 1164–1168.
34. Sperker B *et al.* The role of beta-glucuronidase in drug disposition and drug targeting in humans. *Clin Pharmacokinet* 1997; 33: 18–31.
35. Pasqualini JR, Chetrite GS. Recent insight on the control of enzymes involved in estrogen formation and transformation in human breast cancer. *J Steroid Biochem Mol Biol* 2005; 93: 221–236.